Iraqi Journal for Computer Science and Mathematics
Journal Homepage: http://journal.esj.edu.iq/index.php/IJCM
e-ISSN: 2788-7421 p-ISSN: 2958-0544

Impact of Couple Stress with Rotation on Walters, B Fluid in Porous Medium

Zainab A.Jaafar[1], Mizal H.Thawi[1], Liqaa Z.Hummady[2]

[1]Department of Mathematics, College of Computer Science and Mathematics, University of Tikrit, Tikrit, Iraq
[2]Department of Mathematics, College of Science, University of Baghdad, Baghdad, Iraq

*Corresponding Author: Zainab A.Jaafar

DOI: https://doi.org/10.52866/ijcsm.2023.02.02.017
Received January 2023 ; Accepted march 2023; Available online May 2023

ABSTRACT: This study investigates the peristaltic flow of Walter's B fluid through an asymmetric channel using a couple stress model and a porous material. The constitutive equation is used to model mas balance, motion, trapped phenomena, velocity distribution, and pressure gradient. A wavelength with a low Remolds number assumption is used in the flow analysis, and the perturbation method is used to provide an accurate solution. The impact of various parameters on the velocity distribution and pressure gradient of the confined phenomenon has been learned. The numbers presented here are a graphical representation of these parameters.

Keywords: Peristaltic flow; Walter's B; Couple stress; Rotation.

1. INTRODUCTION

Peristaltic pumping is a type of pumping that is used when a variety of complex rheological fluids can be easily transported from one location to another. This principle of pumping is known as peristaltic. Peristaltic action is responsible for the motions of the small intestine, which are crucial to the proper functioning of the digestive system. Since they are in charge of combining food with digestive juices, breaking down large chunks into smaller ones, bringing it to the surface for nutrient absorption, and driving food along the gastrointestinal tract. Examples include crude oil extraction from petroleum products, food mixing, and blood flow., all of which have been investigated by the references. [1]–[3].

In comparison to Newtonian fluids, non-Newtonian fluids are seen to be more significant and acceptable for use in engineering and biology. Viscoelastic fluid is a non-Newtonian fluid, which contains both viscous and elastic peristaltic [4].

The magneto hydrodynamic (MHD) phenomenon is characterized by an interaction between the hydrodynamic and boundary layer and the electromagnetic filed. The studies of boundary layer flow of viscous and non-Newtonian fluids have received much attention because of their extensive application in the filed metallurgy and chemical engineering. Such investigation of magneto hydrodynamic (MHD) flows are very important industrially and have application in different areas such as petroleum products and metallurgical processes; it is now wellbeing known that in technological application the non-Newtonian fluids are more application than the Newtonian fluids [5].

This research looks into the heat transmission via a porous media and the motion of a magneto hydrodynamic (MHD) non-Newtonian fluid in an inclined symmetric channel. Additionally, the Walter,s B fluid model is implemented via constitutive equations. The mathematical modeling is developed with a constant magnetic field at an angle to the vertical.
Because pair stress fluid has a mechanism to represent rheological complicated fluids like liquid crystals and human blood, studying couple stress fluid is particularly helpful in understanding a variety of physical issues. Peristaltic transfer of pair stress fluid has been studied recently recently by [6], [7] .

For the aforementioned cases, Walter's B fluid with its low limiting viscosity at low shear rates and short memory coefficient is the most appropriate model. Walter's B fluid received a great deal of attention [8]–[13] from an industrial perspective, but only from a physiological one. Researchers [14]looked at the peristaltic transport of a non-Newtonian Walter's B fluid through a porous media in an asymmetric, inclined conduit. As seen in [15], nonlinear peristaltic transport was used to move a porous medium through an angled conduit. Researchers in [16] studied peristaltic blood flow in a magnetic field through irregular conduits. The influence of rotation and starting

*Corresponding author: zainabali611@tu.edu.iq

load on the peristaltic flow of an incompressible fluid was studied by the authors [16]. The investigation of the effects of an angled magnetic field and the heat transfer from an asymmetric channel on hyperbolic tangent peristaltic flow with a porous medium in [17]. Effects of the rotation on the mixed convection heat transfer analysis for the peristaltic transport of viscoelastic fluid in asymmetric channel.in [18]

The goal of this research is to discuss the impact that an inclined magnetic field has on the peristaltic motion of Walter's B fluid. Because of its incompressibility, it fills an asymmetric channel. Parameters including rotation, density, wave amplitude, and channel taper are varied. Variations in the confined phenomenon, velocity distribution, and pressure gradient were also studied using varied values of the parameters.

2. PROBLEM DESCRIPTION

Assume the peristaltic transport of Walters B of an incompressible of tow dimensional in asymmetric channel considering width d1+d2 with electrically conduction fluid through a porous medium. The flow is produced by endless sinusoidal waves that repeat at a fixed speed c along the channel walls. As a result, the symmetric channel has variable wave amplitudes, phase angles, and channel widths.
Here is the modeling of the wall geometries

$$\overline{H}_1(\bar{x},\bar{t}) = d_1 + a_1 \sin[\frac{2\pi}{\lambda}(\bar{x} - c\bar{t})] \text{ upperwall,} \quad (1)$$

$$\overline{H}_2(\bar{x},\bar{t}) = -d_2 - a_2 \sin[\frac{2\pi}{\lambda}(\bar{x} - c\bar{t}) + \Phi] \text{ lowerwall,} \quad (2)$$

where d_1 , d_2 , a_1 , a_2, λ , c, Φ are the wave's amplitude, length, and velocity, Φ is the phase difference various in the range ($0 \le \Phi \le \pi$). Choose the tow dimension system, $\overline{X}$ along centerline channel, while $\overline{Y}$ is transverse to it. This demonstrates that a symmetric channel with out-of-phase waves is represented by a value of Φ=0 , whereas when Φ= π. The waves are in phase. Further a_1 , a_2 , d_1 , d_2, and Φ satisfies the condition.

$$a_1^2 + a_2^2 + 2a_1a_2\cos(\Phi) \le (d_1 + d_2)^2 . \quad (3)$$

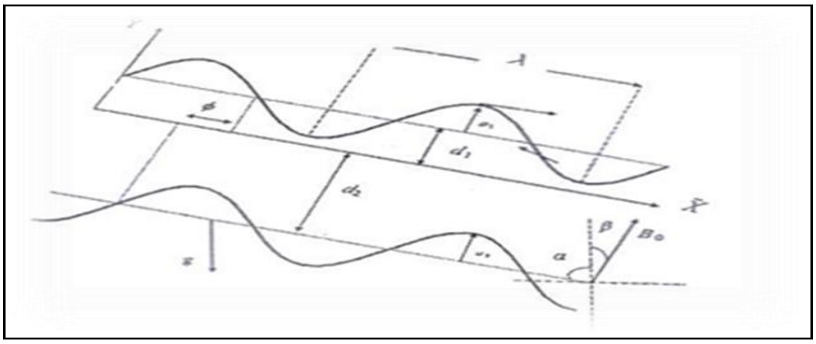

FIGURE 1. visual representation of the issue

3.THE CONSTITUTION EQUATION

Using a laboratory frame ($\bar{x}, \bar{y}$), the continuity and momentum partial differentials of the flow's constitutional equation are written as:

$$\frac{\partial \bar{u}}{\partial \bar{x}} + \frac{\partial \bar{v}}{\partial \bar{y}} = 0 \quad (4)$$

On x-axis

$$\rho(\frac{\partial}{\partial \bar{t}} + \bar{u}\frac{\partial}{\partial \bar{x}} + \bar{v}\frac{\partial}{\partial \bar{y}})\bar{u} - \rho\Omega(\Omega\bar{u} + 2\frac{\partial \bar{v}}{\partial \bar{t}}) = -\frac{\partial \bar{p}}{\partial \bar{x}} + \frac{\partial}{\partial \bar{x}}\bar{T}_{\bar{x}\bar{x}} + \frac{\partial}{\partial \bar{y}}\bar{T}_{\bar{x}\bar{y}} - \sigma B_0^2 \cos\beta^* \quad (5)$$

$$(\bar{u}\cos\beta^* - \bar{v}\sin\beta^*) - \mu\frac{\bar{u}}{\bar{k}} - K_0\nabla^4\bar{u}$$

On y-axis

$$\rho(\frac{\partial}{\partial \bar{t}}+\bar{u}\frac{\partial}{\partial \bar{x}}+\bar{v}\frac{\partial}{\partial \bar{y}})\bar{v}-\rho\Omega(\Omega\bar{u}+2\frac{\partial\bar{u}}{\partial\bar{t}})=-\frac{\partial\bar{p}}{\partial\bar{y}}+\frac{\partial}{\partial\bar{x}}\bar{T}_{\bar{x}\bar{y}}+\frac{\partial}{\partial\bar{y}}\bar{T}_{\bar{y}\bar{y}}+ \tag{6}$$
$$\sigma B_0^2\sin\beta^*(\bar{u}\cos\beta^*-\bar{v}\sin\beta^*)-\mu\frac{\bar{v}}{\bar{k}}-K_0\nabla^4\bar{v}$$

The stress component are given

$$\bar{\tau}_{\bar{x}\bar{x}}=2\mu\bar{u}_{\bar{x}}-K_0[2\bar{u}_{\bar{x}\bar{x}}+2\overline{uu}_{\overline{xx}}+2\bar{v}_{\bar{x}}\bar{u}_{\bar{y}}-2\bar{v}_{\bar{x}}^2-4\bar{u}_{\bar{x}}^2] \tag{7}$$
$$\bar{\tau}_{\bar{x}\bar{y}}=\mu(\bar{u}_{\bar{y}}+\bar{v}_{\bar{x}})-K_0[\bar{u}_{\overline{yt}}+\bar{v}_{\overline{xt}}+\overline{uu}_{\overline{yx}}+\overline{uv}_{\overline{xx}}+\overline{uv}_{\overline{yy}}+$$
$$\overline{vv}_{\overline{xy}}-3\bar{u}_{\bar{x}}\bar{u}_{\bar{y}}-3\bar{v}_{\bar{x}}\bar{v}_{\bar{y}}-\bar{v}_{\bar{y}}\bar{u}_{\bar{y}}-\bar{u}_{\bar{x}}\bar{v}_{\bar{x}}] \tag{8}$$
$$\bar{\tau}_{\overline{yy}}=2\mu\bar{v}_{\bar{y}}-K_0[2\bar{v}_{\overline{yt}}+2\overline{uv}_{\overline{yx}}+2\overline{vv}_{\overline{yy}}-2\bar{v}_{\bar{x}}\bar{u}_{\bar{y}}-2\bar{u}_{\bar{y}}^2-4\bar{v}_{\bar{y}}^2] \tag{9}$$

And

$$\nabla^2=\delta^2\frac{\partial^2}{\partial x^2}+\frac{\partial^2}{\partial y^2}\ ,\qquad \nabla^4=(\nabla^2)^2$$

Where the $\bar{\tau}_{\overline{xx}},\bar{\tau}_{\overline{xy}},\bar{\tau}_{\overline{yy}}$ are the elements of extra stress tensor. And $\rho,\bar{u},\bar{v},\bar{y},\bar{p},\mu,k_0,\bar{k},B_0$ are the fluid density ,axial velocity , the transverse velocity, the transverse coordinate , the pressure, the viscosity , the material constant, the permeability parameter, and the constant magnetic field, The electrical conductivity is unsteady in natural peristaltic motion. Peristaltic motion is unsteady in nature, we can assume steady by using transformation from laboratory frame ($\bar{x},\bar{y}$) to wave frame ($\bar{X},\bar{Y}$) which defined as:

$$\bar{X}=\bar{x}+c\bar{t},\ \bar{Y}=\bar{y}\ ,\ \bar{U}=\bar{u}+c\ ,\bar{V}=\bar{v}\ ,\ \bar{P}(\bar{X},\bar{Y})=\bar{P}(\bar{x},\bar{y},\bar{t}) \tag{10}$$

The velocity elements represented by $\bar{U},\bar{V}$ and $\bar{P}$ of the pressure in the wave frame.

The following non-dimensional quantities are arranged in order to carry out the non-dimensionalanalysis:

$$\bar{x}=\lambda x\quad ,\bar{y}=d_1y,\bar{u}=cu\quad ,\bar{v}=cv\delta\quad ,\bar{H}_1=h_1d_1,\bar{H}2=h_2d_1,\bar{p}=\frac{p\mu c\lambda}{d_1^2}$$
$$\bar{k}=k\,d_1^2,Re=\frac{\rho cd_1}{\mu},\delta=\frac{d_1}{\lambda},Ha=d_1\sqrt{\frac{\sigma}{\mu}}B_0,\bar{\tau}=\frac{\tau\mu c}{d1}, \tag{11}$$
$$K=\frac{k_0c}{\mu d_1},\bar{t}=\frac{t\lambda}{c},\alpha=d_1\sqrt{\frac{\mu}{K_0}}$$

Where (Ha) is the Hartman number, (Re) is the Reynold number,(δ) is the wave number, (K) is the viscoelastic parameter,(α) represent couple stress parameter.

Thereafter, in light of Equation (11), Equations. (3) to (9) takes the form

$$\frac{\partial u}{\partial x}+\frac{\partial v}{\partial y}=0 \tag{12}$$

$$\mathrm{Re}\,\delta(\frac{\partial u}{\partial t}+u\frac{\partial u}{\partial x}+v\frac{\partial u}{\partial y})-\frac{\rho\Omega^2d_1^2}{\mu}u-\frac{2\delta^2}{c\mu}\frac{\partial v}{\partial t}=-\frac{\partial p}{\partial x}+\delta\frac{\partial\tau_{xx}}{\partial x}+\frac{\partial\tau_{xy}}{\partial y}-$$
$$Ha^2\cos\beta^*(u\cos\beta^*-v\delta\sin\beta^*)-\frac{u}{k}-\frac{1}{\alpha^2}(\delta^4\frac{\partial^4}{\partial x^4}+\delta^2\frac{\partial^4}{\partial x^2\partial y^2}+\frac{\partial^4}{\partial y^2})u \tag{13}$$

$$\mathrm{Re}\,\delta^3(\frac{\partial v}{\partial t}+u\frac{\partial v}{\partial x}+v\frac{\partial v}{\partial y})-\frac{\rho\Omega^2d_1^2}{\mu}v\delta^2-\frac{2\delta^2}{c\mu}\frac{\partial u}{\partial t}=-\frac{\partial p}{\partial y}+\delta^2\frac{\partial\tau_{xy}}{\partial x}+\delta\frac{\partial\tau_{yy}}{\partial y}+$$
$$Ha^2\delta\sin\beta^*(u\cos\beta^*-v\delta\sin\beta^*)-\delta\frac{v}{k}-\frac{\delta}{\alpha^2}(\delta^4\frac{\partial^4}{\partial x^4}+\delta^2\frac{\partial^4}{\partial x^2\partial y^2}+\frac{\partial^4}{\partial y^4})v \tag{14}$$

The components of extra stress tenser of walter's B are listed below

$$\tau_{xx} = 2\delta u_x - 2\delta^2 K[uu_{xx} + vu_{xy} - v_x u_y - \delta^2 v_x^2 - 2u_x^2] \tag{15}$$

$$\tau_{xy} = (u_y + \delta^2 v_x) - \delta K[uu_{yx} + \delta^2 uv_{xx} + vu_{yy} + \delta^2 vv_{xy} - 3u_y u_x \\ -3\delta^2 v_x v_y - v_y u_y - \delta^2 u_x v_x] \tag{16}$$

$$\tau_{yy} = 2\delta v_y - K[2\delta^2 uv_{yx} + 2\delta^2 vv_{yy} - 2u_y^2 - 2\delta^2 u_y v_x - 4\delta^2 v_y^2] \tag{17}$$

The velocity elements are linked to the stream function (ψ) by the relationships

$$U = \frac{\partial\psi}{\partial y}\ ,\ V = -\frac{\partial\psi}{\partial x} \tag{18}$$

Substituted Equation (10) and Equation (18) in Equations (13-17), respectively

$$\mathrm{Re}\,\delta(\psi_y \frac{\partial\psi y}{\partial x} - \psi_x \frac{\partial\psi y}{\partial y}) - \frac{\rho\Omega^2 d_1^2}{\mu}\psi y + \frac{2\delta^2}{c\mu}\frac{\partial\psi x}{\partial t} = -\frac{\partial p}{\partial x} + \delta\frac{\partial\tau_{xx}}{\partial x} + \frac{\partial\tau xy}{\partial y} - Ha^2\cos\beta^* \\ ((\psi_y - 1)\cos\beta^* + \delta\psi_x \sin\beta^*) - \frac{1}{k}\psi_y - \frac{1}{\alpha^2}(\delta^4\frac{\partial^4}{\partial x^4} + \delta^2\frac{\partial^4}{\partial x^2\partial y^2} + \frac{\partial^4}{\partial y^4})\psi_y \tag{19}$$

$$\mathrm{Re}\,\delta^3(\psi_y \frac{\partial\psi x}{\partial x} - \psi_x \frac{\partial\psi x}{\partial y}) - \frac{\rho\Omega^2 d_1^2\delta^2}{\mu} - \frac{2\delta^2}{c\mu}\frac{\partial\psi y}{\partial t} = -\frac{\partial p}{\partial y} + \delta^2\frac{\partial\tau_{xy}}{\partial x} + \delta\frac{\partial\tau yy}{\partial y} + \delta Ha^2\sin\beta^* \\ ((\psi_y - 1)\cos\beta^* + \delta\psi_x \sin\beta^*) + \frac{\delta}{k}\psi_x + \frac{\delta^2}{\alpha^2}(\delta^4\frac{\partial^4}{\partial x^4} + \delta^2\frac{\partial^4}{\partial x^2\partial y^2} + \frac{\partial^4}{\partial y^4})\psi_x \tag{20}$$

$$\tau_{xx} = (2\delta\psi_{xy}) - 2\delta^2 K(\psi_y\psi_{xxy} - \psi_x\psi_{xyy} - 2\psi_{xy}^2 + \\ \psi_{xx}\psi_{yy} + \delta^2\psi_{xx}^2) \tag{21}$$

$$\tau_{xy} = (\psi_{yy} - \delta^2\psi_{xx}) - \delta K(\psi_y\psi_{xyy} - \delta^2\psi_y\psi_{xxx} - \psi_x\psi_{yyy} \\ + \delta^2\psi_x\psi_{xxy} - 2\psi_{xy}\psi_{yy} - 2\delta^2\psi_{xx}\psi_{xy} \tag{22}$$

$$\tau_{yy} = -2\delta\psi_{xy} - K(-2\delta^2\psi_y\psi_{xxy} + 2\delta^2\psi_x\psi_{xyy} - 2\psi_{yy}^2 + \\ 2\delta^2\psi_{xx}\psi_{yy} - 4\delta^2\psi_{xy}^2 \tag{23}$$

Removal of p between Equations (19) and (20) produce

$$\mathrm{Re}\,\delta(\psi_y\frac{\partial}{\partial x} - \psi_x\frac{\partial}{\partial y})\nabla^2\psi + (\frac{\rho\Omega^2 d_1^2\delta^2}{\mu} + \frac{2\delta^2}{c\mu}\frac{\partial}{\partial t})(\psi_x - \psi_y) = \delta[\frac{\partial^2}{\partial x\partial y}(\tau_{xx} - \tau_{yy})] + [\frac{\partial^2}{\partial y^2} - \\ \delta^2\frac{\partial^2}{\partial x^2}]\tau_{xy} - Ha^2\cos^2\beta^*\frac{\partial^2\psi}{\partial y^2} + \delta^2 Ha^2\sin^2\beta^*\frac{\partial^2\psi}{\partial x^2} - \\ -\delta Ha^2\cos\beta^*\sin\beta^*\psi_{xy} - \frac{1}{k}(\psi_{yy} + \delta\psi_{xx}) - \frac{1}{\alpha^2}(\delta^4\frac{\partial^4}{\partial x^4} + \delta^2\frac{\partial^4}{\partial x^2\partial y^2} + \frac{\partial^4}{\partial y^2})\psi_{yy} \\ -\frac{\delta^2}{\alpha^2}(\delta^4\frac{\partial^4}{\partial x^4} + \delta^2\frac{\partial^4}{\partial x^2\partial y^2} + \frac{\partial^4}{\partial y^4})\psi_{xx} \tag{24}$$

The wave frame by the dimensionless boundary conditions:

$$\psi = \frac{F}{2}\ ,\ \frac{\partial\psi}{\partial y} = -1 \quad \text{at} \quad y = h_1. \tag{25}$$

$\psi = \frac{-F}{2}$, $\frac{\partial \psi}{\partial y} = -1$ at y= h_2. (26)

$\frac{\partial \psi}{\partial y} + \beta_1 \frac{\partial^2 \psi}{\partial y^2} = -1$, at $y = h_1$ (27)

$\frac{\partial \psi}{\partial y} - \beta_1 \frac{\partial^2 \psi}{\partial y^2} = -1$ at $y = h_2$ (28)

$\frac{\partial^3 \psi}{\partial y^3} = 0$ at $y = h_1$ (29)

$\frac{\partial^3 \psi}{\partial y^3} = 0$ at $y = h_2$ (30)

The dimensionless time mean flow rate (F) in the wave frame. In the laboratory frame the dimensionless time mean flow rate Q1 is related to F by through the expression:

$Q1 = F + 1 + d.$ (31)

The $h_1(x)$ and $h_2(x)$ the dimensionless forms

$h1(x) = 1 + a \sin x, \ h2(x) = -d - b \sin(x + \Phi),$ (32)

where a ,b, Φ and d satisfy :

$a^2 + b^2 + 2ab\cos(\Phi) \le (1+d)^2.$ (33)

4.THE EMPACT OF COUPLE STRESS

This section provides the link between the viscoelastic and pair stress parameters. Using this connection, we can simplify the problem. The effect of all parameters, such as viscoelastic and pair stress, should be investigated in this study. At begging must find zero-th and first orders solutions, when us the relationship between viscoelastic and couple stress parameters we will find the zero-th order

$K = \frac{K_0 c}{\mu d_1}$ divided by c (34)

$\frac{K}{c} = \frac{K_0}{\mu d_1}$ divided by d_1

$\frac{K}{c d_1} = \frac{K_0}{\mu d_1^2}$ (35)

Then

$\frac{c d_1}{K} = \frac{\mu d_1^2}{K_0}$ (36)

Substitute

$\alpha = d_1 \sqrt{\frac{\mu}{K_0}}$ in to Eq. (32), we get

$\frac{c d_1}{K} = \alpha^2$ and $\frac{1}{\alpha^2} = \frac{K}{c d_1}$ (37)

5.SOLUTION OF THE PROBLE

Substituting Equations(8)-(23) in to Equation (24) and assumption the low Reynolds number and the long wavelength, we often the motion equation in frame of stream function

$\psi_{yyyy} - \frac{1}{\alpha^2} \psi_{yyyyyy} - \zeta^2 \psi_{yy} = 0$ (38)

when

$m^2 = Ha^2 \cos^2 \beta^* + \frac{1}{k}$

$$\zeta = \frac{\rho \Omega^2 d_1^2}{\mu} + m^2$$

The solution of the momentum equation is straight forward and can be written as

$$\psi = \sqrt{2}\left(\frac{\sqrt{2}e^{p_1 y}C1}{p3} + \frac{\sqrt{2}e^{-p_1 y}C2}{p3} + \frac{\sqrt{2}e^{p_2 y}C3}{p4} + \frac{\sqrt{2}e^{-p_2 y}C4}{p4}\right) + C5 + yC6 \quad (39)$$

where

$$P_1 = \frac{\sqrt{\alpha^2 - \sqrt{\alpha^2(\alpha^2 - 4\zeta)}}}{\sqrt{2}}$$

$$P_2 = \frac{\sqrt{\alpha^2 + \sqrt{\alpha^2(\alpha^2 - 4\zeta)}}}{\sqrt{2}} \quad (40)$$

$$P_3 = \sqrt{\alpha^2 - \sqrt{\alpha^2(\alpha^2 - 4\zeta)}}\sqrt{\alpha^2 - \sqrt{\alpha^4 - 4\alpha^2\zeta}}$$

$$P_4 = \sqrt{\alpha^2 + \sqrt{\alpha^2(\alpha^2 - 4\zeta)}}\sqrt{\alpha^2 + \sqrt{\alpha^4 - 4\alpha^2\zeta}}$$

The function C1, C2, C3, C4, C5, C6 are large expression will mention in the end of this work.

$$\frac{\partial p}{\partial x} = \psi_{yyy} - Ha^2 \cos^2 \beta^* (\psi_y - 1) - \frac{\psi_y}{K} - \frac{1}{\alpha^2}\psi_{yyyyy} + \frac{\rho \Omega^2 d_1^2}{\mu}\psi_y \quad (41)$$

6.RESULTS AND DISCUSSION

This section is divided in to sub sections. In the first place, we talk about traps. In the second, we look at the scatterplot of velocities. MATHEMATIC is used to graphically represent the pressure gradients stated in the third.

6.1 TRAPPING SECTION

Peristaltic motion's trapping is an intriguing phenomenon. In essence, it is the closed stream line creation of an internally circulating bolus of fluid. We testing the stream function profile with changing the values of parameters (k, α, β_1, Ha, Ω). The profile of stream lines behavior is increasing on the change for different parameters. Notes that the changing of the stream line and appearing the bolus for every parameter clearly in figures (2,4,5,6,7). Figure (3) We found that when the parameter (*Φ*) value increased, the trapped bolus shrank. The profile of stream line no effect of the size of trapped bolus with increasing the values of parameters (Q, β^*) clearly in figures. (8,9).

6.2 VELOCITY SECTION

The velocity distribution is represented by various properties. The change in velocity for different values of (Ω, α, β_1, Ha, ϕ, K, Q, β^*) is explained in figures (10-17). In figures (10,12) As we increase the various parameters (Ω, Ha), we see that the axial velocity in the channel's middle portion decreases. Whereas the axial velocity increases near the channel wall's edge. As the parameters (K), are increased, the axial velocity in the channel's central region increases, while. figure (11). shows that there is no influence from the channel's edge. As the parameters (α), are increased, the core part of the channel experiences a drop in axial velocity. while no effect of the boundary of channel that is shown in figure (14). The axial velocity decrease in the central region and near the right wall of the channel with increasing the parameter (ϕ), whereas increases near the left wall of the channel that is explained in figure (13). The axial velocity increases near the right wall of the channel with increasing the parameter (β_1), whereas the velocity decreases in the middle and the left wall of channel that is in figure (15). From figures (16,17) shows that there is no effect on the axial velocity with increasing in the value of parameters (Q, β^*).

6.3 PRESSURE GRADIENT

The effect of different values of parameters (K, α, β_1, Ha, Ω, ϕ, Q, β^*) on pressure gradient its clearly in figures (18-25). Figures (18) that ascending values of the parameters (Ω) we see that the pressure gradient has no effect on the area close to the right wall of the channel, but it does increase the area close to the center and the left wall. In figures (19,22,23) the pressure gradient increases of the channel with increasing the parameters (K, β_1, Ha). As the values of the parameters (α) are increased, the pressure gradient at the channel's wall boundary rises, while on effect of the central region that is explained in figure (21). Notes that the pressure gradient no effect of the channel with increasing of the parameters (Q, β^*) shown it in figures (24,25). The pressure gradient increases near the left wall of the channel with increasing the parameters (*Φ*), while on effect of the central region and decreases near the right wall of the channel that is explained in figure (20).

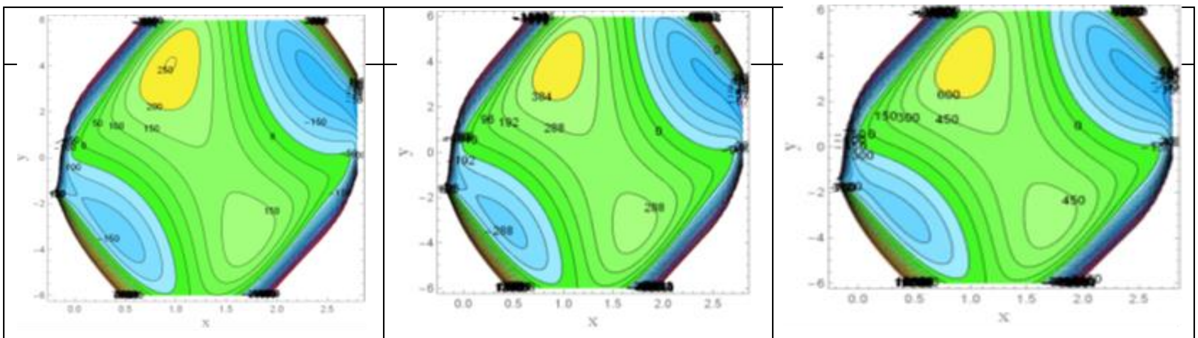

FIGURE 2. (a)K=1.5, (b)K=2, (c)K=2.5, $\phi = 0.4$, α=1.5,β_1=2, Ha=0.1, a=7, b=7, d^*=0.08,
=0.5

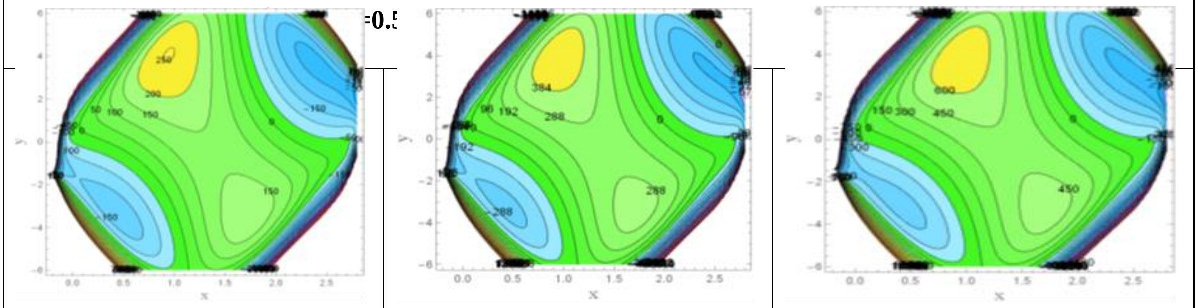

FIGURE 3. K=1.5,(a) $\phi = 0.4$, (b) $\phi = 0.6$, (c) $\phi = 0.8$, α=1.5,β_1=2,Ha=0.1, a=7, b=7, d^*=0.08,
=0.5

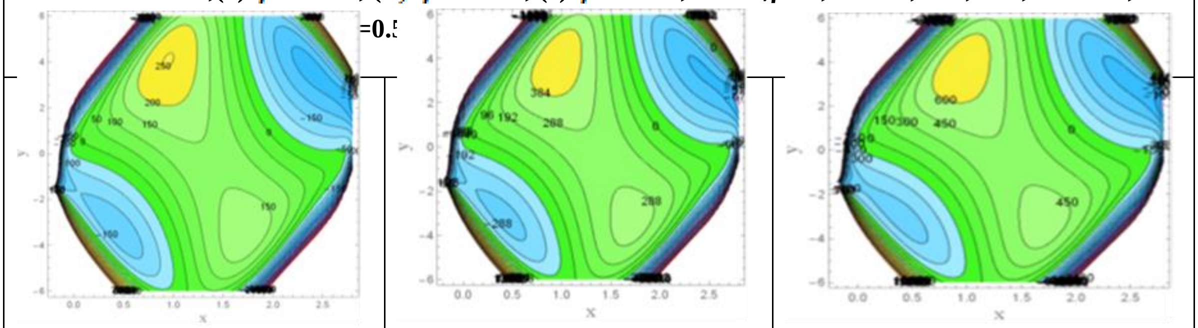

FIGURE 4. K=1.5, $\phi = 0.4$, (a

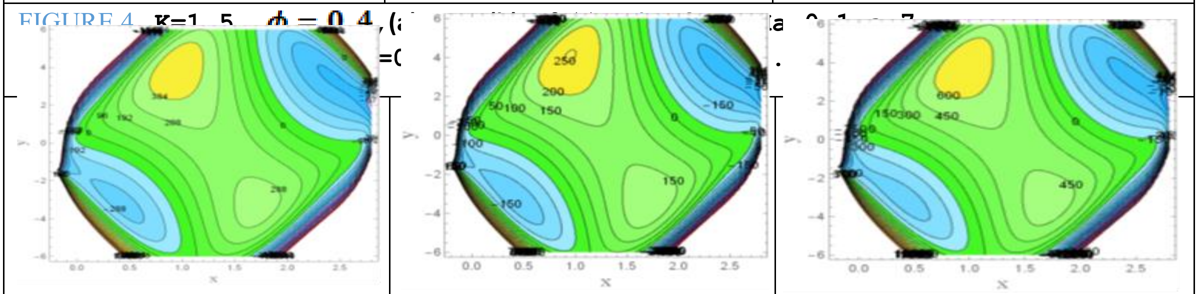

FIGURE 5. K=1.5, ϕ=0.4,α=1.5,(a) β_1=2,(b), β_1=3, (c)β_1 =4, Ha=0.1,a=7,b=7, d^*=0.08, F_0=0.3, F_1=0,Ω=6,d1=0.1,μ=0.5, ρ=0.6, Q=1.5,β*=pi/6

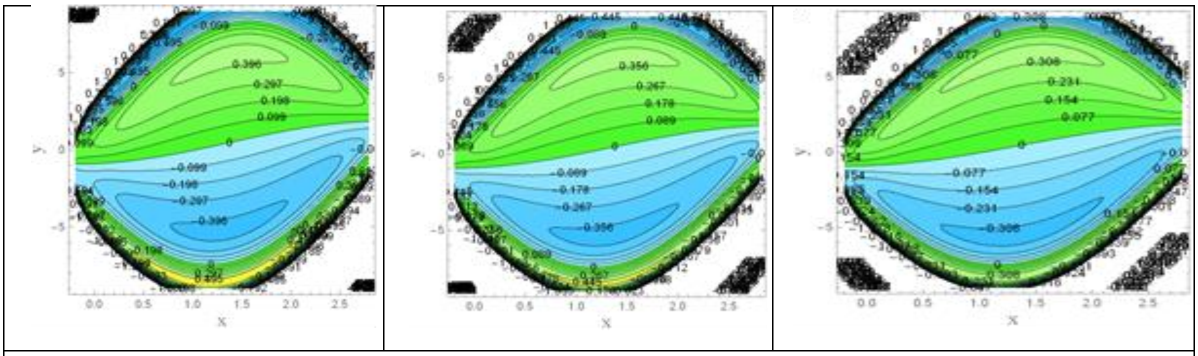

FIGURE 6. K=1.5, ϕ=0.4,α=1.5,β_1=2, (a) Ha=0.1, (b) Ha=0.8, (c) Ha=1.4, a=7, b=7, d^*=0.08, F_0=0.3, F_1=0, Ω=6, d1=0.1, μ=0.5, ρ=0.6, Q=1.5, β^*=pi/6

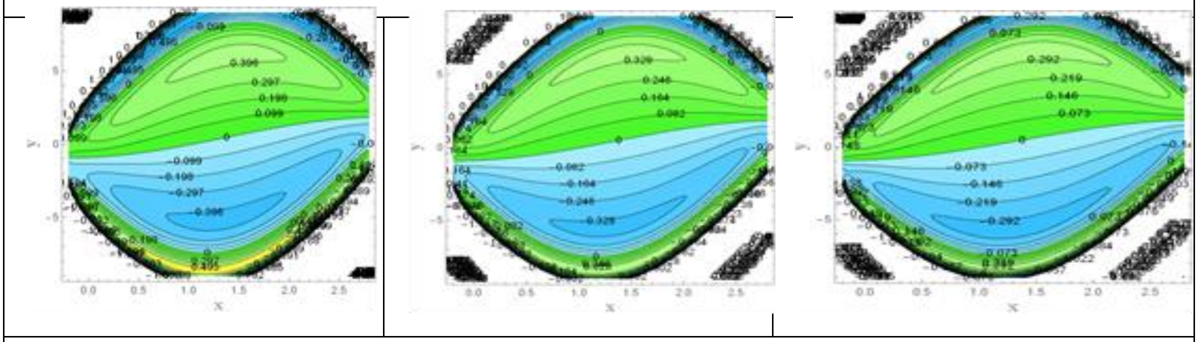

FIGURE 7. K=1.5, ϕ=0.4,α=1.5,β_1=2,Ha=0.1, a=7, b=7, d^*=0.08, F_0=0.3, F_1=0 (a) Ω=6, (b) Ω=11 , (c) Ω=14, d1=0.1, μ=0.5, ρ=0.6, Q=1.5, β^*=pi/6

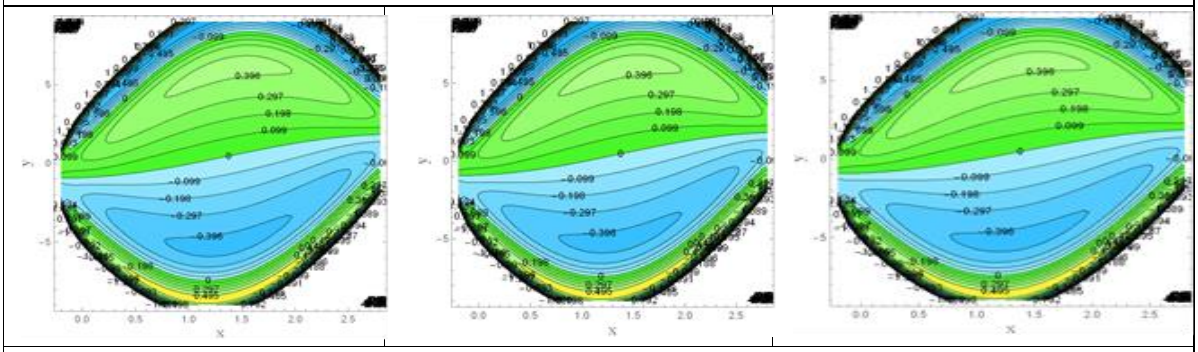

FIGURE 8. K=1.5, ϕ=0.4,α=1.5,β_1=2,Ha=0.1,a=7,b=7, d^*=0.08, , F_0=0.3, F_1=0, Ω=6,d1=0.1,μ=0.5, ,ρ=0.6,(a)Q=1.5,(b)Q=1.8,(c)Q=2,β^*=pi/6

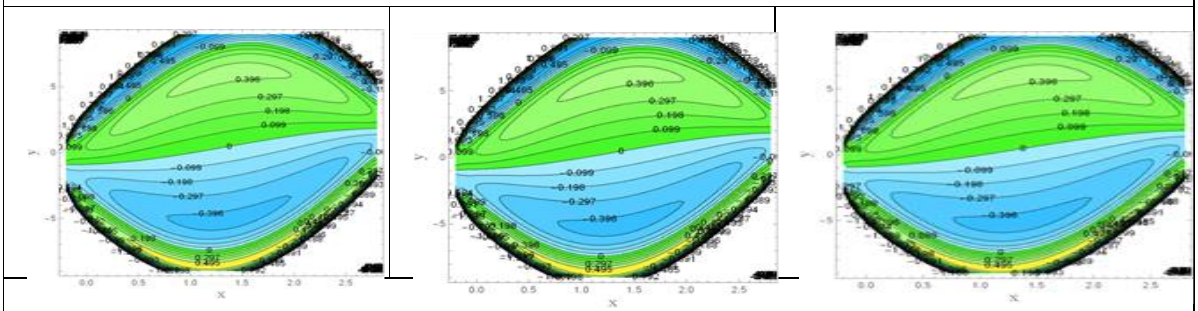

FIGURE 9. K=1.5, ϕ=0.4,α=1.5,β_1=2,Ha=0.1,a=7,b=7, d^*=0.08, , F_0=0.3, F_1=0, Ω=6,d1=0.1, μ=0.5, ,ρ=0.6,Q=1.5,(a)β^*=pi/6,(b) β^*=pi/4, (c) β^*=pi/2

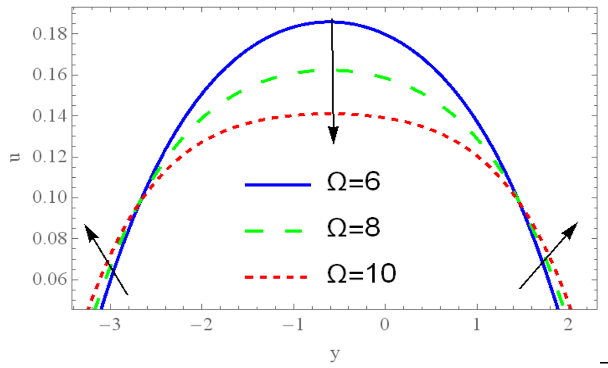

FIGURE 10. **variation of velocity for different values of Ω when**
K=4.5, ϕ =0.4, α=1.5,β1=2,Ha=0.1,a=3,b=4 ,d*=0.8,F0=0.3,d1=0.1, μ=0.5, ρ=0.6 ,Q=1.5, β*=pi/6,x=1

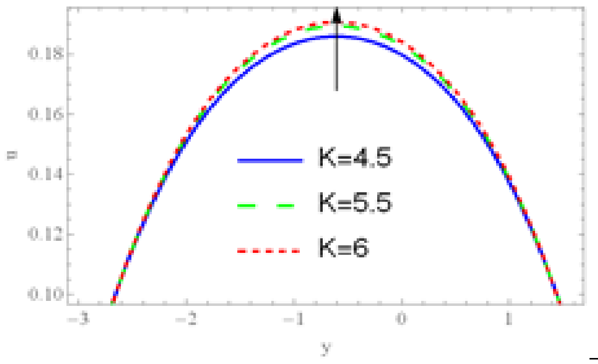

FIGURE 11. **variation of velocity for different values of K when**
ϕ =0.4, α=1.5,β1=2,Ha=0.1,a=3,b=4 ,d*=0.8,F0=0.3,d1=0.1, Ω=6, μ=0.5, ρ=0.6 ,Q=1.5, β*=pi/6,x=1

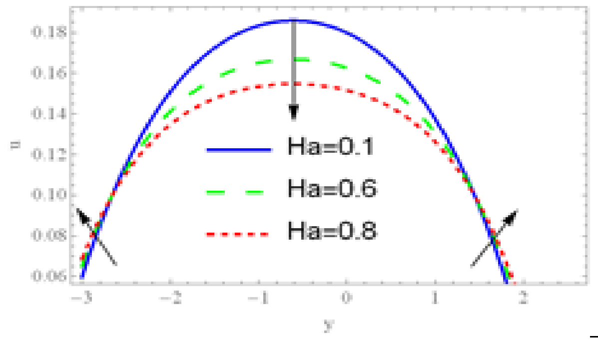

FIGURE 12. **variation of velocity for different values of Ha when K=4.5, ϕ =0.4, α=1.5,β1=2,a=3,b=4 ,d*=0.8,F0=0.3,d1=0.1, Ω=6,μ=0.5, ρ=0.6 ,Q=1.5, β*=pi/6,x=1**

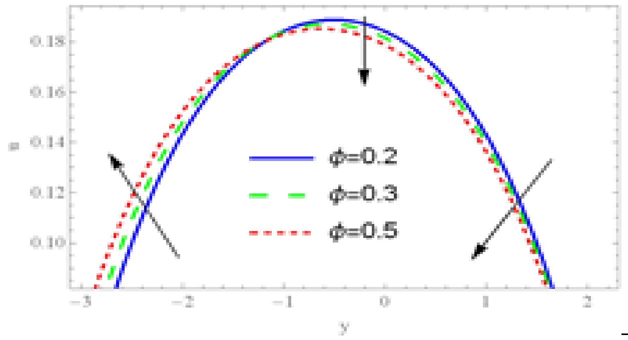

FIGURE 13. **variation of velocity for different values of ϕ when**
K=4.5, α=1.5,β1=2,Ha=0.1,a=3,b=4 ,d*=0.8,F0=0.3,d1=0.1, Ω=6,μ=0.5, ρ=0.6 ,Q=1.5, β*=pi/6,x=1

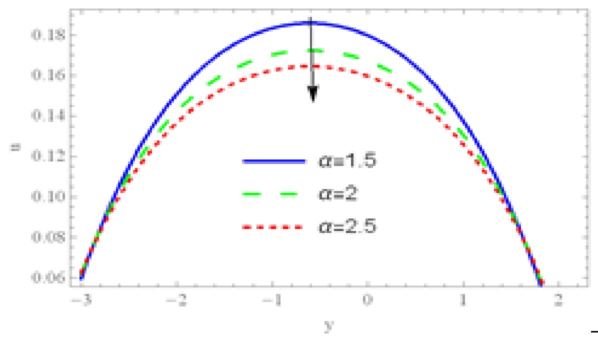

FIGURE 14. **variation of velocity for different values of α when K=4.5,ϕ=0.4,β1=2,Ha=0.1,a=3,b=4,d*=0.8,F0=0.3 ,Ω=6,d1=0.1,μ=0.5,ρ=0.6,Q=1.5, β^*=pi/6,x=1**

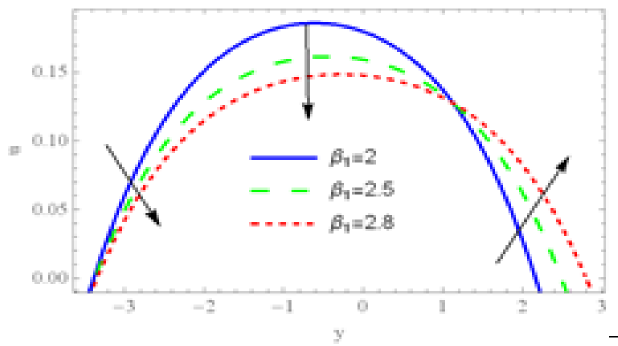

FIGURE 15. **variation of velocity for different values of β1 when K=4.5, ϕ=0.4,α=1.5,Ha=0.1,a=3,b=4,d*=0.8,F0=0.3 ,Ω=6,d1=0.1,μ=0.5,ρ=0.6,Q=1.5, β^*=pi/6,x=1**

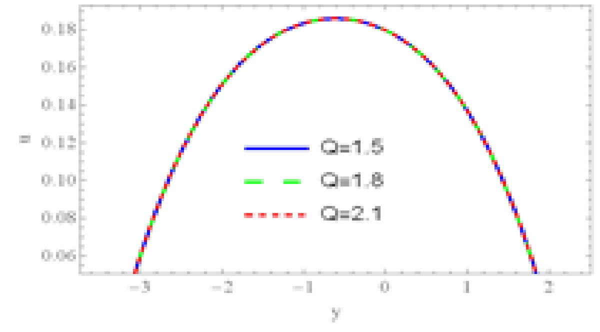

FIGURE 16. **variation of velocity for different values of Q when**
K=4.5, ϕ=0.4,α=1.5,Ha=0.1,β_1=2,a=3,b=4,F0=0.3 ,Ω=6, d^*=0.8,d1 =0.1, μ =0.5, ρ=0.6, β^*=pi/6,x=1

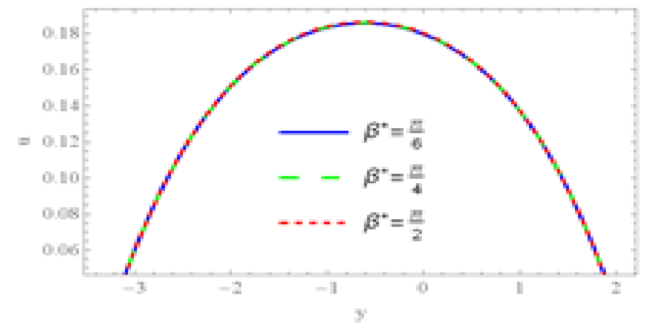

FIGURE 17. **variation of velocity for different values of β^* when**
K=4.5, ϕ=0.4,α=1.5,Ha=0.1,β_1=2,a=3,b=4,F0=0.3 ,Ω=6, d^*=0.8,d1 =0.1, μ =0.5, ρ=0.6, Q=1.5,x=1

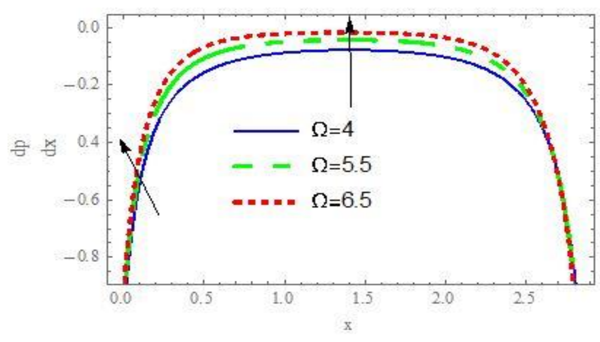

FIGURE 18.Variation of pressure gradient for different values of Ω when
K=1.5,ϕ=0.3, α=1.5,β1=2,Ha=0.1,a=4 ,b=4, d^*=0.01, F0=0.3 ,d1=0.1,μ=0.5 ,ρ=0.6,Q=1.5, β^*=o.4,y=0.001

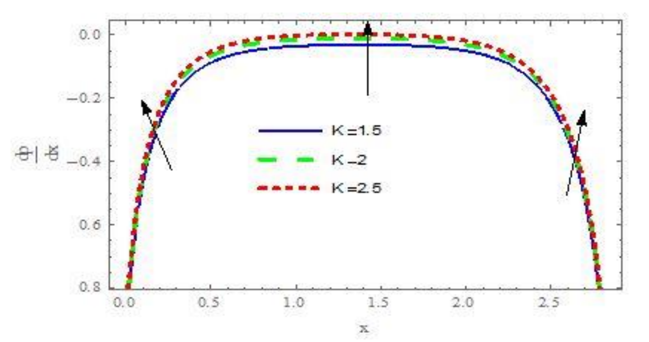

FIGURE 19.Variation of pressure gradient for different values of K when
ϕ=0.3, α=1.5,β1=2,Ha=0.1,a=4,b=4, d^*=0.01,F0=0.3 ,d1=0.1,Ω=6,μ=0.5,ρ=0.6,Q=1.5, β^*=o.4,y=0.001

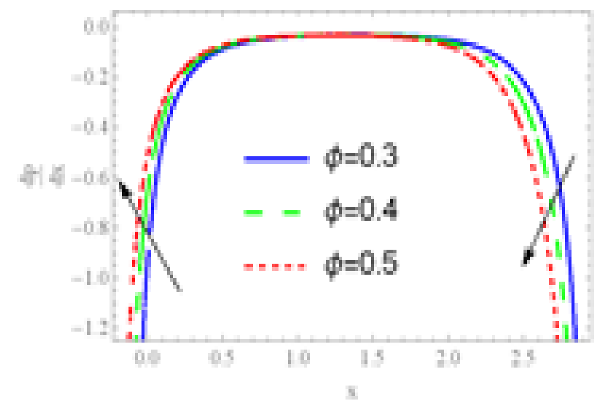

FIGURE 20. **Variation of pressure gradient for different values of ϕ when**
K=1.5, α=1.5,β1=2,Ha=0.1,a=4,b=4, d^*=0.01 ,F0=0.3 ,d1=0.1,Ω=6,μ=0.5,ρ=0.6,Q=1.5, β^*=o.4,y=0.001

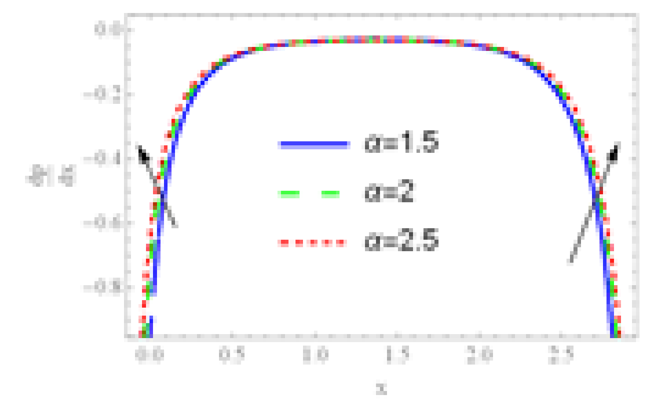

FIGURE 21. **Variation of pressure gradient for different values of α when**
K=1.5, ϕ=0.3,β1=2,Ha=0.1,a=4,b=4, d^*=0.01, F0=0.3,d1=0.1,Ω=6 ,μ=0.5,ρ=0.6,Q=1.5, β^*=o.4,y=0.001

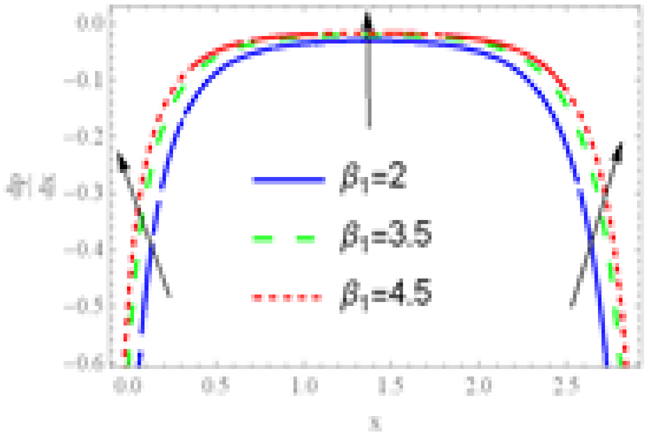

FIGURE 22. Variation of pressure gradient for different values of β_1 when
K=1.5, ϕ=0.3,α=1.5,Ha=0.1,a=4,b=4, d^*=0.01, F0=0.3,d1=0 .1,Ω=6,μ=0.5,ρ=0.6,Q=1.5, β^*=o.4,y=0.001

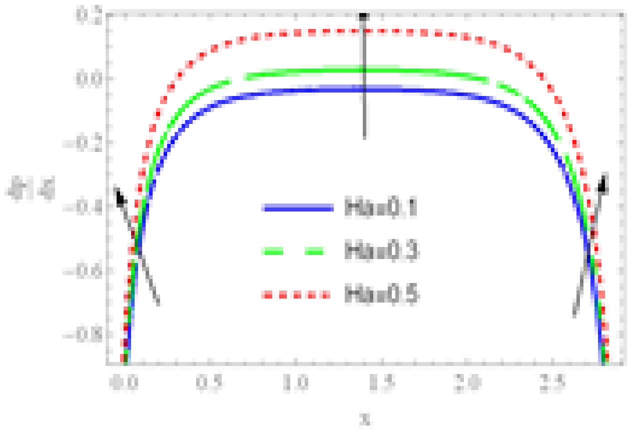

FIGURE 23.Variation of pressure gradient for different values of Ha when
K=1.5, ϕ=0.3,α=1.5,β_1=2,a=4,b=4, d^*=0.01, F0=0.3,d1=0. 1,Ω=6,μ=0.5,ρ=0.6,Q=1.5, β^*=o.4,y=0.001

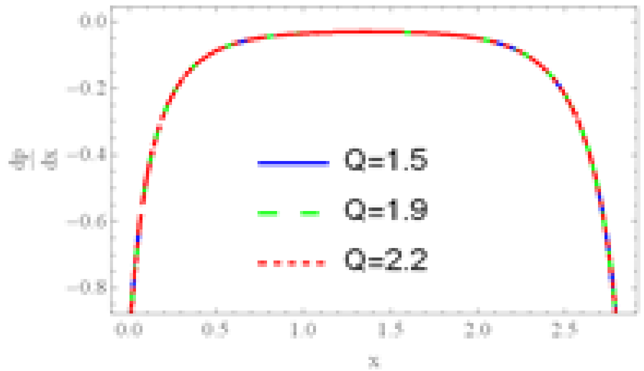

FIGURE 24.Variation of pressure gradient for different values of Q when
K=1.5, ϕ=0.3,α=1.5,β_1=2,Ha=0.1,a=4,b =4,F0=0.3 ,d^*=0.01,Ω=6,d1=0.1,μ=0.5, ρ=0.6, β^*=o.4,y=0.001

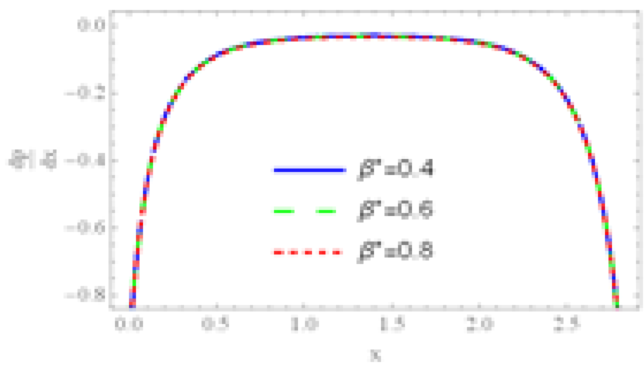

FIGURE 25.Variation of pressure gradient for different values of β^* when
K=1.5, ϕ=0.3,α=1.5,β_1=2,Ha=0.1,a=4,b =4,F0=0.3 ,d^*=0.01,Ω=6,d1=0.1,μ=0.5, ρ=0.6, Q=1.5,y=0.001

7. CONCLUTION

The study focused on how rotating in an asymmetric channel and porous medium affects Walters' B fluid with couple stress and an angled magnetic field. Special attention was placed in this inquiry on studying trapping phenomena, velocity distribution and pressure gradient using a simple analytical solution.

-In case of stream function the trapped bolus size increases with increasing the value of parameters $(K, Ha, \alpha, \beta 1, \Omega)$.

- We saw that when the value of the parameter (Φ) increased, the size of the trapped bolus shrank.

- The amount of the trapped bolus has no impact on the stream line profile as parameters (Q, β^*) values increase.

- The axial velocity decreases in the core part of the channel as each parameter (Ω, Ha) increases, whereas the axial velocity increases along the channel wall's parameter.

- As the fluid parameter (K) are raised, the axial velocity increases in the channel's center and no effect of the boundary of channel.

- As the fluid parameter (α) are raised, the axial velocity decreases in the channel's center and no effect of the boundary of channel.

- When the parameter (ϕ) is raised, the axial velocity increases near the channel's right wall and drops in the channel's middle and on its left.

- As the parameter (ϕ) is increased, the axial velocity increases near the left wall of the channel and drops in the central region and towards the right wall.

- Increasing either parameter's value (Q, β*) has no noticeable impact on the axial velocity.

- Using these parameters (Ω), we see that the pressure gradient has no effect on the area close to the right wall of the channel, but it does increase the area close to the center and the left wall.

- As the parameters (K, β1, Ha) are raised, the pressure gradient in the channel rises.

- The pressure gradient at the channel wall's boundary increases as the parameters (α) are increased, while on effect of the central region and the pressure gradient no effect of the channel with increasing of the parameters (Q, β*).

- The pressure gradient increases near the left wall of the channel with increasing the parameters (Φ), while on effect of the central region and decreases near the right wall.

Funding

None

ACKNOWLEDGEMENT

Acknowledgements and Reference heading should be left justified, bold, with the first letter capitalized but have no numbers. Text below continues as normal.

CONFLICTS OF INTEREST

The author declares no conflict of interest.

REFERENCES

[1] T. W. Latham, "Fluid motions in a peristaltic pump." Massachusetts Institute of Technology, 1966.

[2] E. F. Elshehawey and A. M. F. Sobh, "Peristaltic viscoelastic fluid motion in a tube," *Int. J. Math. Math. Sci.*, vol. 26, no. 1, pp. 21–34, 2001.

[3] M. Rashid, K. Ansar, and S. Nadeem, "Effects of induced magnetic field for peristaltic flow of Williamson fluid in a curved channel," *Phys. A Stat. Mech. its Appl.*, vol. 553, p. 123979, 2020.

[4] S. Akram, A. Razia, and F. Afzal, "Effects of velocity second slip model and induced magnetic field on peristaltic transport of non-Newtonian fluid in the presence of double-diffusivity convection in nanofluids," *Arch. Appl. Mech.*, vol. 90, pp. 1583–1603, 2020.

[5] N. Ali, T. Hayat, and M. Sajid, "Peristaltic flow of a couple stress fluid in an asymmetric channel," *Biorheology*, vol. 44, no. 2, pp. 125–138, 2007.

[6] A. M. Abdulhadi and A. H. Al-Hadad, "Effects of rotation and MHD on the Nonlinear Peristaltic Flow of a Jeffery Fluid in an Asymmetric Channel through a Porous Medium," *Iraqi J. Sci.*, vol. 57, no. 1A, pp. 223–240, 2016.

[7] S. Ravikumar, G. P. Rao, and R. S. Prasad, "Peristaltic flow of a couple stress fluid in a flexible channel under an oscillatory flux," *Int. J. Appl. Math Mech*, vol. 6, no. 13, pp. 58–71, 2010.

[8] S. Bariş, "Steady three-dimensional flow of a Walter's B'fluid in a vertical channel," *Turkish J. Eng. Environ. Sci.*, vol. 26, no. 5, pp. 385–394, 2002.

[9] S. BARIŞ, "Steady flow of a Walter's B'viscoelastic fluid between a porous elliptic plate and the ground," *Turkish J. Eng. Environ. Sci.*, vol. 26, no. 5, pp. 403–418, 2002.

[10] T. Muhammad, H. Ahmad, U. Farooq, & A. Akgül. (2023). Computational Investigation of Magnetohydrodynamics Boundary of Maxwell Fluid Across Nanoparticle-Filled Sheet. Al-Salam Journal for Engineering and Technology, 2(2), 88–97. https://doi.org/10.55145/ajest.2023.02.02.011

[11] J.-H. He, "Approximate analytical solution for seepage flow with fractional derivatives in porous media," *Comput. Methods Appl. Mech. Eng.*, vol. 167, no. 1–2, pp. 57–68, 1998.

[12] S. G. Mohiddin, V. R. Prasad, S. V. K. Varma, and O. A. Bég, “Numerical study of unsteady free convective heat and mass transfer in a Walters-B viscoelastic flow along a vertical cone,” *Int. J. Appl. Math. Mech.*, vol. 6, no. 15, pp. 88–114, 2010.

[13] M. M. Nandeppanavar, M. S. Abel, and J. Tawade, “Heat transfer in a Walter’s liquid B fluid over an impermeable stretching sheet with non-uniform heat source/sink and elastic deformation,” *Commun. Nonlinear Sci. Numer. Simul.*, vol. 15, no. 7, pp. 1791–1802, 2010.

[14] S. Nadeem and N. S. Akbar, “Peristaltic flow of Walter’s B fluid in a uniform inclined tube,” *J. Biorheol.*, vol. 24, no. 1, pp. 22–28, 2010.

[15] K. S. Mekheimer, “Non-linear peristaltic transport of magnetohydrodynamic flow in an inclined planar channel,” *Arab. J. Sci. Eng.*, vol. 28, no. 2, pp. 183–202, 2003.

[16] K. S. Mekheimer, “Peristaltic flow of blood under effect of a magnetic field in a non-uniform channels,” *Appl. Math. Comput.*, vol. 153, no. 3, pp. 763–777, 2004.

[17] S. A. Abdulla and L. Z. Hummadya, “Inclined magnetic field and heat transfer of asymmetric and Porous Medium Channel on hyperbolic tangent peristaltic flow,” *Int. J. Nonlinear Anal. Appl.*, vol. 12, no. 2, pp. 2359–2371, 2021.

[18] H. N. Mohaisen and A. M. Abedulhadi, “Effects of the Rotation on the Mixed Convection Heat Transfer Analysis for the Peristaltic Transport of Viscoplastic Fluid in Asymmetric Channel,” *Iraqi J. Sci.*, pp. 1240–1257, 2022.